AJNR

FLAIR Diffusion-Tensor MR Tractography: Comparison of Fiber Tracking with Conventional Imaging

Ming-Chung Chou, Yi-Ru Lin, Teng-Yi Huang, Chao-Ying Wang, Hsiao-Wen Chung, Chun-Jung Juan and Cheng-Yu Chen

AJNR Am J Neuroradiol 2005, 26 (3) 591-597
http://www.ajnr.org/content/26/3/591

FLAIR Diffusion-Tensor MR Tractography: Comparison of Fiber Tracking with Conventional Imaging

Ming-Chung Chou, Yi-Ru Lin, Teng-Yi Huang, Chao-Ying Wang, Hsiao-Wen Chung, Chun-Jung Juan, and Cheng-Yu Chen

***BACKGROUND AND PURPOSE*: Partial volume with CSF is known to contaminate the quantification of white matter anisotropy depicted by diffusion tensor imaging (DTI). We hypothesized that the FLAIR technique helps to improve DTI white matter tractography in the normal adult brain by eliminating CSF partial volume effects.**

***METHODS:* Seven healthy adults aged 23–37 underwent both conventional and FLAIR DTI at 1.5T. Each subject was imaged five times. Neural fiber tractography was performed with both sequences by using two algorithms: a voxel-based method (EZ-tracing) with global seed points and another based on subvoxel tractography (tensor deflection) by using manual encircling of local seed points. Total volume of the fibers tracked was compared for the two types of images.**

***RESULTS:* Fiber tracking was substantially most successful on FLAIR DTI near the lateral ventricles and the sulci, where CSF partial volume effects were likely present. Minor false tracts on FLAIR images, possibly due to a reduced signal-to-noise ratio, were found in regions relatively free of CSF contamination; however, they did not affect tracking of major periventricular white matter bundles, such as those related to the corpus callosum or the corona radiata. When we excluded false tracts, the FLAIR technique depicted an average of 17% more fibers in volume than conventional DTI in the periventricular regions ($P < .0005$, paired Student *t* test).**

***CONCLUSION:* Despite the reduction of signal-to-noise ratio and longer imaging times, FLAIR improved tractography by eliminating CSF partial volume effects.**

White matter tractography by means of diffusion tensor imaging (DTI) has raised clinical attention, because tractography can noninvasively reveal functional connectivity of the neuronal pathways (1, 2). One potential problem in the quantitative derivation of diffusion-related parameters from MR imaging data is contamination from CSF (3–5). Because CSF has a relatively large diffusion coefficient compared with that of the brain parenchyma, partial volume effects in the periventricular regions and in the sulci could result in overestimation of the apparent diffusion coefficient (ADC) by about 15–30% (3). In addition, because CSF diffusion is largely isotropic, ADC overestimation could lead to underestimation of diffusion anisotropy in regions of brain parenchyma prone to partial volume effects (4–6).

Inaccuracy in the derivation of diffusion-related parameters due to CSF contamination can be eliminated with the suppression of CSF signals by using the fluid-attenuated inversion recovery (FLAIR) technique incorporated into a diffusion imaging sequence (4, 5, 7, 8). However, questions remain whether similar arguments hold true for DTI white matter tractography (3–5). In particular, the accuracy of fiber tracking algorithms strongly relies on the image signal-to-noise ratio (SNR) in addition to the anisotropy measurements (9). Because FLAIR diffusion imaging has an intrinsically lower SNR than that of conventional diffusion imaging with the same imaging time (5, 6), use of the FLAIR technique in diffusion tractography could result in a trade-off between the ben-

Received April 20, 2004; accepted after revision July 6.

From the Department of Electrical Engineering, National Taiwan University (M.-C.C., Y.-R.L., T.-Y.H., C.-Y.W., H.-W.C., C.-J.J.), and the Department of Radiology, Tri-Service General Hospital (M.-C.C., C.-Y.W., H.-W.C., C.-J.J., C.-Y.C.), Taipei, Taiwan, ROC.

Supported in part by the National Science Council under grant NSC-90-2213-E-002-102 Taiwan, ROC.

Presented at the 12th Annual Meeting of the International Society for Magnetic Resonance in Medicine, July 14–21, 2004, Kyoto, Japan.

Address reprint requests to Cheng-Yu Chen, MD, Department of Radiology, Tri-Service General Hospital and National Defense Medical Center, No 325, Sec 2, Cheng-Kung Road, Neihu 114, Taipei, Taiwan, ROC.

efits of reduced partial volume effects and the inherently inferior SNR. Therefore, the purpose of our study was to investigate the effects of FLAIR CSF suppression on white matter tractography in the normal adult brain. Specifically, we hypothesized that FLAIR DTI could depict a larger volume of neural fiber tracts than that obtained with conventional DTI methods.

Methods

Subjects

Seven healthy volunteers (aged 23–37 years, all men) participated in this study. None of these volunteers had history of neurologic diseases, and all of their brain MR images were normal. Our institutional review board approved the entire study, including the MR imaging protocol, and all subjects provided written informed consent. MR examinations were performed using a 1.5T MR system (Siemens Vision; Erlangen, Germany) with a single-channel circularly polarized head coil. The maximal gradient strength was 25 mT/m.

Image Acquisition

Axial conventional DTIs were acquired by using a spin-echo echo-planar imaging sequence. The diffusion-sensitizing gradients were applied along six directions: (+x)–(+y), (+x)–(−y), (+y)–(+z), (+y)–(−z), (+z)–(+x), and (+z)–(−x), with the diffusion weighting factor $b = 1400$ s/mm^2, plus one reference image with $b = 0$ s/mm^2. Spatial misregistrations due to eddy current effects were removed by using a twice-refocused spin-echo technique (10) with bipolar gradient waveforms (11). Imaging parameters, unless otherwise noted, were as follows: TR/TE/NEX = 5000/120/4, FOV= 24 cm, section thickness = 3–5 mm (no intersection gap), and matrix size = 128 × 128. Total imaging time was 2 minutes 20 seconds, with 16 sections acquired.

FLAIR DTIs were obtained by using the same spin-echo echo-planar imaging sequence as stated before, with the exception that a section selective 180° inversion radio-frequency pulse was added before the 90° excitation pulse. Multisection acquisition was achieved with sequential-order section interleaving during the TI. The section thickness for the inversion pulse was adjusted to about 1.4 times that of the excitation pulse to minimize incomplete CSF suppression due to through-section CSF flow (12). To obtain gapless sections and to simultaneously avoid cross-talk for the inversion pulses, the image acquisition process was completed in two steps: first for odd-numbered sections and second for even-numbered sections. These steps increased the total imaging time by a factor of 2. In our study, the TI was 2300 ms, with TR increased to 9000 ms. All other imaging parameters were kept identical to those used in the conventional DTI sequence as stated before. The total imaging time for 16 sections was 2 minutes 6 seconds for each signal acquired. Magnitude reconstruction was used for the FLAIR images, as all tissues other than CSF have already relaxed to positive longitudinal magnetization at this long TI. In addition, the use of real component reconstruction provides no advantages in terms of SNR (13).

Each subject underwent five imaging sessions with both conventional and FLAIR DTI. Therefore, the total number of examinations was 35 for the seven subjects.

Data Analysis

After data acquisition, image calculations were performed on a personal computer after digital transfer of the DTIs from the MR operating console. The diffusion tensor was calculated on a voxel-by-voxel basis by using the known relationship with the b matrix (14). The principal fiber direction was derived from the diffusion tensor as the eigenvector associated with the largest eigenvalue. Fractional anisotropy (FA) was computed (6, 15), and FA maps were generated as gray-scale images. In addition, vector-encoded FA maps were created to assist in visualization; on these maps, every voxel in the gray-scale FA maps was overlaid with a color-coded line segment representing the principal fiber direction.

Two methods were used for fiber tracking. The first one was the EZ-tracing algorithm (16), which can be viewed as a voxel-based counterpart of other subvoxel tractography methods (2, 9). In EZ-tracing, global tracking was used (i.e., with seed points of the tracts were automatically searched within the entire 3D imaging region). Thresholds for fiber connection were set as follows: FA > 0.2, angle between principal eigenvectors in adjacent voxels $<18°$, and angle between principal eigenvector and the vector connecting neighboring voxels $<18°$ within a 5 × 5-pixel window (16). For a fair comparison to address only the effects of CSF suppression by using FLAIR imaging, these settings were kept identical for both the conventional DTI and FLAIR DTI. The resulting fiber tracts in yellow color were superimposed on the original echo-planar images acquired with $b = 0$ s/mm^2.

The second tractography method was a subvoxel fiber-tracking algorithm based on tensor deflection (17), with seed points manually selected to start automatic tracking of the fibers. The stepping parameter for the tensor deflection algorithm was set at 0.5 voxel, meaning that the tracked fiber was allowed to "turn" its orientation twice within one single image voxel (17).

The purpose for using different tractography algorithms was twofold. First, the output of the EZ-tracing algorithm was a 2D single-section display on which the possible false tracts could be better visualized, whereas the output of the subvoxel algorithm yielded 3D colored fiber bundles superimposed on the original MR images in gray scale, facilitating visual examination at different viewing angles. Second, the large amount of fiber tracts detected with the global EZ-tracing algorithm helped in detecting all possible false tracts within the entire imaging region, whereas the local fiber-tracking method based on tensor deflection allowed one to see whether the possible false tracts affected the examination of major neural pathways. Specifically in the tensor deflection algorithm, we adopted the fundamental assumption of all tractography algorithms, which treated adjacent voxels by showing consistent directions in their principal eigenvectors as being really connected by some neural fibers. Therefore, any tracts oriented consistently with the major pathways were regarded as true tracts, because the presence of noise could only result in increased directional deviations. Those inconsistent with knowledge of normal anatomy were regarded as false.

Comparison of the effects of CSF suppression on tractography was carried out for the voxel-based EZ-tracing algorithm by computing the total volume of the fibers found in selected regions of interest near the lateral ventricles. To simplify matters, the total volume of fibers detected was defined as the total number of voxels that were assigned as containing some neural fibers. Also (as its rationale will become clear later), a restriction of regions of interest to a rectangular volume about 8 × 6 × 4 cm encompassing the lateral ventricles was used in this comparison. In this manner, the reported increase in the total fiber volumes for FLAIR versus conventional DTI tractograms reflected the overall influence from both an elimination of partial volume effects and a reduction in SNR but not from the apparent false tracts. As a consequence, the comparison results reported were mostly confined to the periventricular white matter tracts related to the corpus callosum and the corona radiata.

We chose not to compare total fiber volume by using the tensor deflection tractography algorithm because tensor deflection tractography is by its nature a subvoxel algorithm (17), meaning that the computation of total number of voxels is meaningless when a certain voxel of interest contains some

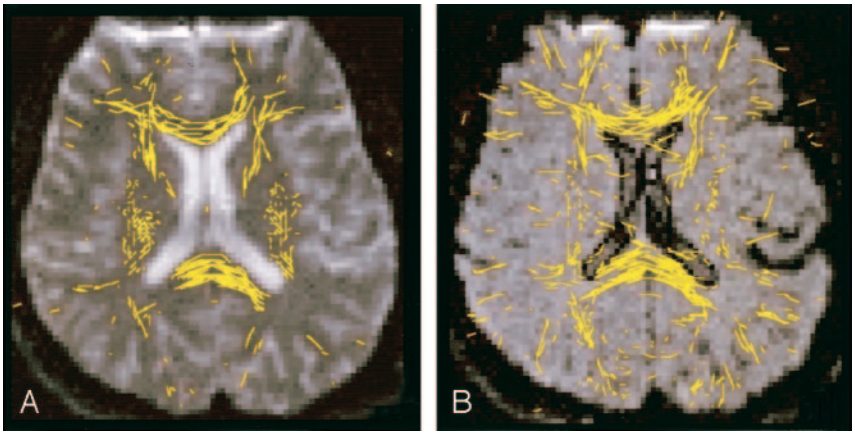

FIG 1. White matter EZ-tracing tractograms in a 24-year-old man. Images show the white matter tracts (*yellow*) superimposed on images obtained with $b = 0$ s/mm^2.

A, Tractogram obtained by using conventional DTI.

B, Tractogram obtained by FLAIR DTI shows a larger area of white matter fiber tracts in both the genu and the splenium of the corpus callosum.

locally tortuous fiber tracts. In other words, fiber volume computation for the tensor deflection algorithm may likely reflect indirect influences from the subvoxel tractography algorithm itself, in addition to the effects from FLAIR CSF suppression.

Results

Figure 1 shows the comparison of a section of white matter tractograms (obtained with global EZ-tracing) by using conventional DTI (Fig 1A) and FLAIR DTI (Fig 1B), respectively. Tracking was substantially more successful on FLAIR DTI in the regions of the corpus callosum and near the sulci, where the partial volume effects with CSF were likely to be present. (As a side note, some yellow fibers in Figure 1 that appeared relatively isolated usually mean that they were connected to voxels in an adjacent section.)

Figure 2 shows the anterior aspects of an image section, demonstrating the difference between conventional (Fig 2A, C, and E) and FLAIR (Fig B, D and F) DTI tractograms in terms of partial volume effects. FA maps (Fig 2C and D) were displayed at the same window level to allow for a side-by-side comparison of the FA values (i.e., brightness). We clearly observed a larger amount of white matter tracts in the corpus callosum on the FLAIR DTI tractogram (Fig 2B) than on the conventional DTI tractogram (Fig 2A). On conventional DTI tractograms, partial volume effects with adjacent CSF in the lateral ventricles resulted in underestimation of FA at the edge of the corpus callosum, compared with the FLAIR DTI tractogram (Fig 2D vs. C). The underestimation of FA in conventional DTI further led to uncertainty of the major fiber orientations in the genu of the corpus callosum (Fig 2E).

Arranged in a similar manner, Figure 3 shows the posterior aspect of the same image section as Figure 2, demonstrating tractographic differences due both to partial volume and SNR effects. Although the FLAIR DTI tractogram again showed more tracts in the splenium of the corpus callosum than the conventional DTI tractogram, some amount of false tracts was found in the occipital lobes (Fig 3B). These tracts were regarded as artificial because they continuously traversed across the cerebral midline where no crossing fibers should exist in the anatomically normal brain. Closer examination indicated a noisier appearance of the FA map obtained by using FLAIR DTI (Fig 3D), which possibly led to incidentally consistent orientations of the eigenvectors (Fig 3F).

Although false tracts were sometimes found in the FLAIR tractograms, the locations and occurrence of these tracts were not highly reproducible, suggesting random effects possibly due to noise. In our initial experience, scattered false tracts tended to appear in regions prone to susceptibility-related geometric distortions, such as the superior frontal gyri. In addition, the false tracts identified on the tractograms by using global seed points appeared focal and had no obvious connections with major fiber tracts that are consistent with our knowledge of normal neuroanatomy. Figure 4 shows the white matter tracts originating from only the entire corpus callosum on a left anterior oblique view superimposed on the original axial image. The fiber tracts from FLAIR DTI (Fig 4B) were visually larger in volume than those obtained with conventional DTI (Fig 4A), suggesting that a reduction in partial volume effects by using FLAIR helped in identifying white matter fibers near the lateral ventricles. Visual verification on these images showed that the focal false tracts in FLAIR DTIs (as seen in Fig 3) seemed to exhibit minimal influence on the major white matter tracts when the seed points were specifically located.

Figure 5 shows the comparison of total volumes of fibers tracked from conventional versus FLAIR DTIs. FLAIR DTI depicted significantly larger volumes of fiber tracts than conventional DTI for all our subjects. Because some minor false tracts were found near the superior frontal gyrus and in the occipital lobes, we restricted our regions of interest in a central rectangular volume about $8 \times 6 \times 4$ cm^3, so that the comparison was confined to periventricular white matter tracts mostly in the corpus callosum and the corona radiata. In addition, we browsed through all individual sections of the tractograms to ensure that false tracts were not included in the comparison. On average, about 17% additional volume of fiber tracts were detected on FLAIR DTI compared with conventional DTI. The group difference was statistically significant.

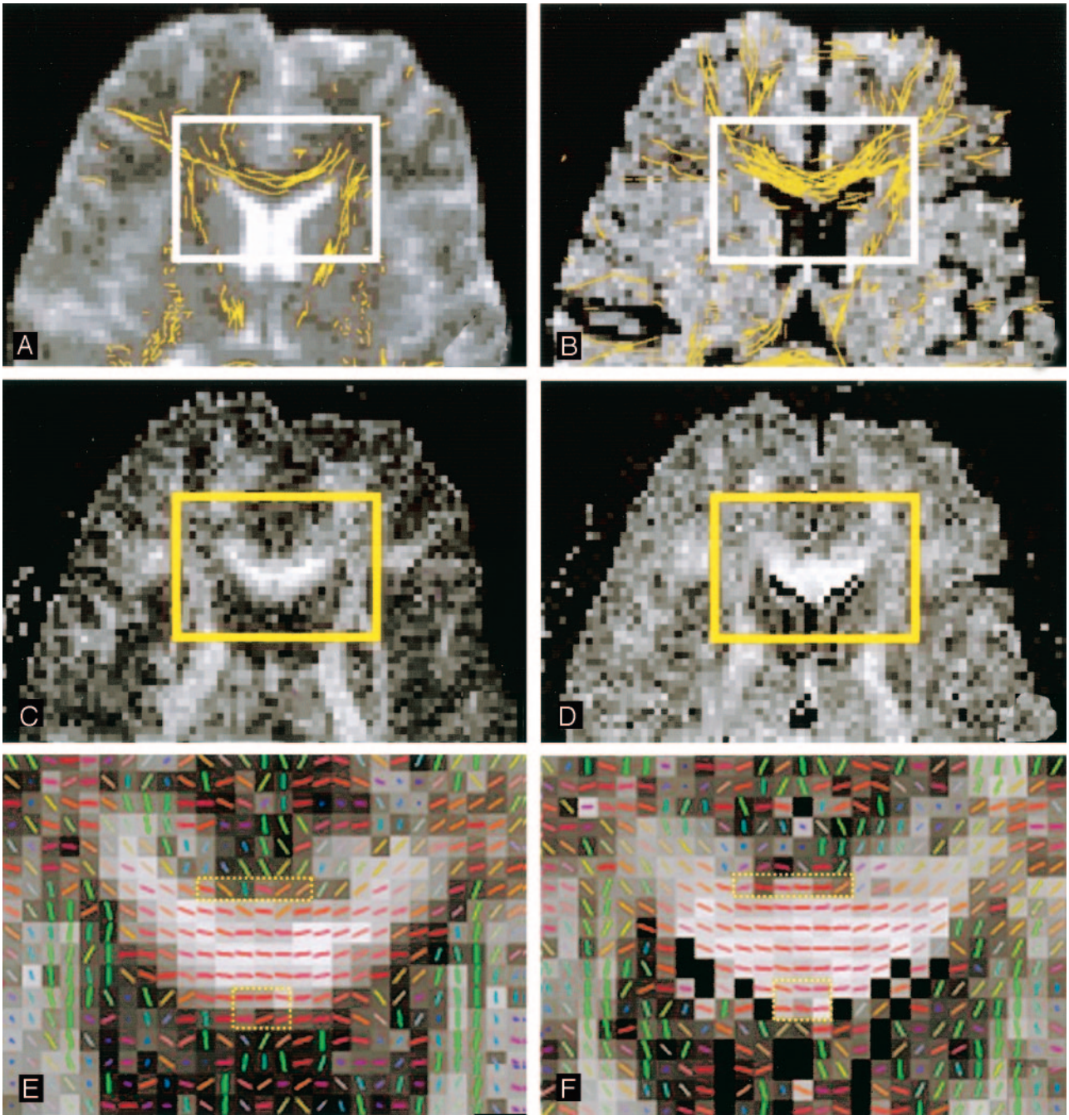

FIG 2. Anterior aspects of an image section obtained in an 23-year-old man show white matter tracts superimposed on images *A–F* magnified from the rectangular region-of-interest (*solid rectangles*). Partial volume effects near adjacent CSF lead to underestimation of FA in the genu of the corpus callosum on conventional DTI (*left* column and *dashed rectangles* in *E*.) Note the less consistent fiber directions and the darker gray level, which indicates lower FA values. These effects account for the smaller amount of fibers found with the tracking algorithm on conventional DTI than on FLAIR DTI (*right* column, *dashed rectangles* in *F*). Note the more consistent fiber directions and the brighter gray level, which indicates higher FA values.

A and *B*, Images obtained with $b = 0$ s/mm^2 by using the EZ-tracing algorithm.

C and *D*, FA maps in gray scale displayed in the identical window level.

E and *F*, Vector-encoded FA maps. *Red* indicates left-right; *green*, anteroposterior; and *blue*, superoinferior.

Discussion

White matter tractography is potentially a useful technique for assessing neural fiber connectivity (18) in traumatic axonal injury (19), brain maturation (20), and so forth (21). In the presence of CSF partial volume effects, a seemingly reduced volume of the tracked fibers might mimic partially destroyed integrity or underdevelopment of the neural fiber architecture, leading to misleading findings. Our results, therefore, have important implications in that they address the efficacy of the FLAIR DTI technique by eliminating the problems from CSF partial volume effects, particularly in regions near the ventricles and the sulci. Consequently, when brain regions prone to

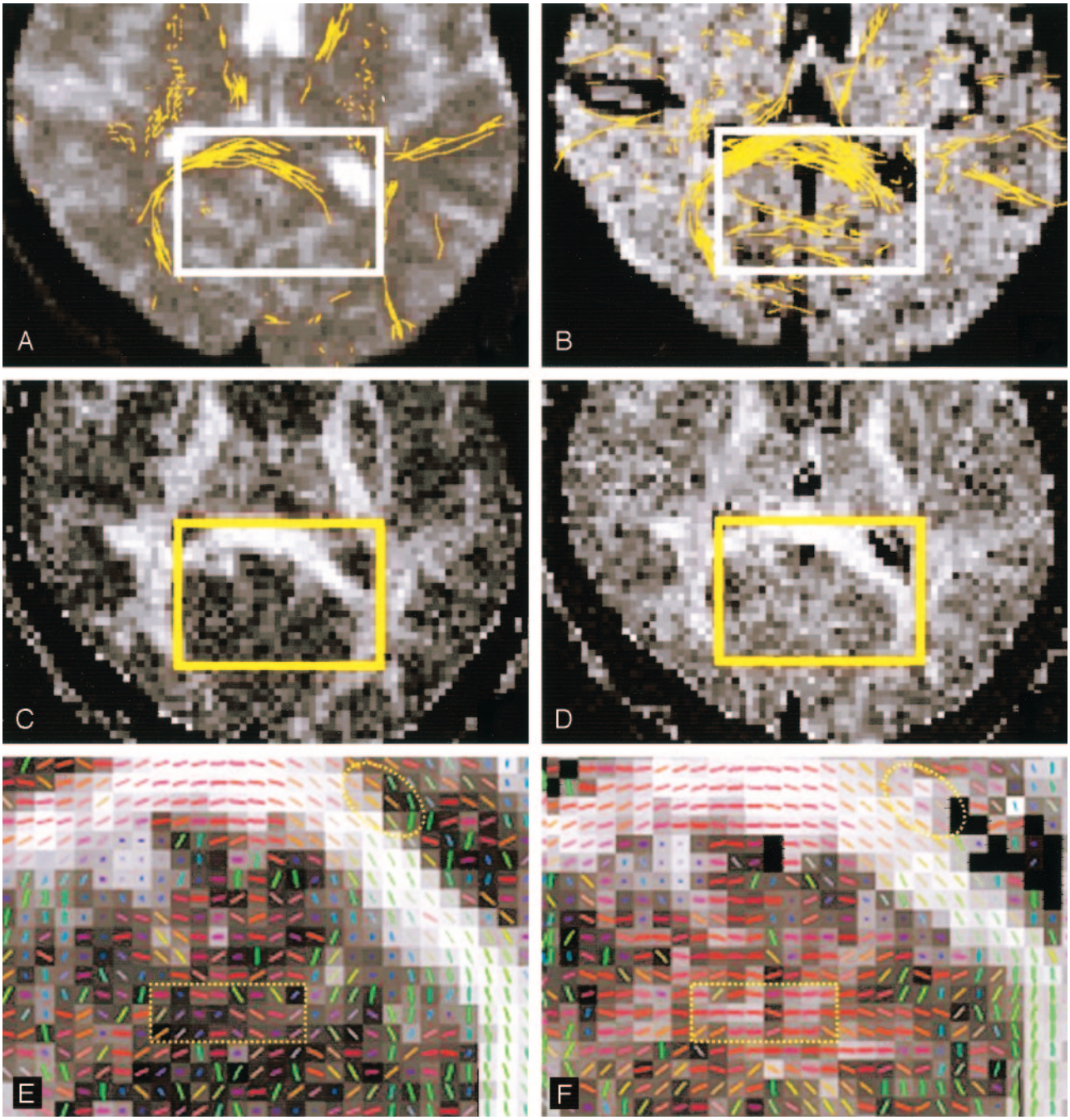

FIG 3. Posterior aspects of the same image section as in Figure 2 show white matter tracts superimposed on the images in *A–F* magnified from the rectangular region-of-interest (*solid rectangles*). Although the FLAIR DTI tractogram shows more tracts in the splenium of the corpus callosum (*B* and *dashed oval* in *F,* with more consistent fiber directions) than the conventional DTI tractogram (*A* and *dashed oval* in *E*, with less consistent fiber direction near the lateral ventricle), false tracts are found in the occipital lobes (*B*).

A and *B*, Images obtained with $b = 0$ s/mm^2 by using the EZ-tracing algorithm.

C and *D*, FA maps in gray scale displayed in identical window level obtained by using conventional (*C*) and FLAIR DTI (*D*). *D* is noisier than *C*, suggesting uncertainty in FA values.

E and *F*, Vector-encoded FA maps show that the false tracts in *B* are due to incidentally consistent orientations of the eigenvectors (*rectangle* in *F*), which is absent in *E* (*rectangle* in *E*). *Red* indicates left-right; *green*, anteroposterior; and *blue*, superoinferior.

CSF contamination are of clinical interest, FLAIR DTI should be the method of choice for white matter tractography.

Our results suggest that an elimination of CSF partial volume effects by using FLAIR is helpful for white matter tractography in regions near the ventricles and brain surfaces. Specifically, an average of 17% increase in the volume of neural fiber tracts could be found by using FLAIR images rather than conventional DTIs. In the corpus callosum near the lateral ventricles, the increase in fiber tract volumes found on FLAIR images was due to FA values higher than those on conventional DTI. This finding is in good agreement with results of previous studies,

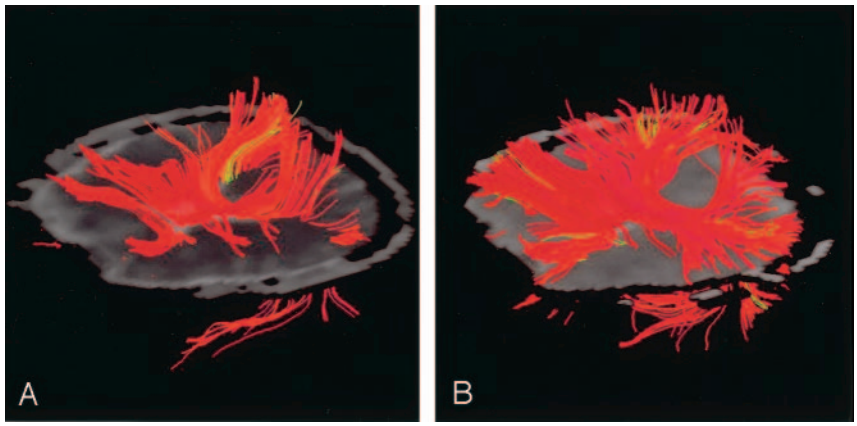

FIG 4. Left anterior oblique views of white matter tracts (*colored* region) superimposed on the images in *A* and *B*. Images were obtained in another 23-year-old man by using the subvoxel tractography algorithm based on tensor deflection with identical parameter settings. Fiber tracts on FLAIR DTI were visually larger in volume than those on conventional DTI.

A, Original axial image (*gray*) obtained with seed points placed in the corpus callosum for conventional DTI.

B, FLAIR DTI.

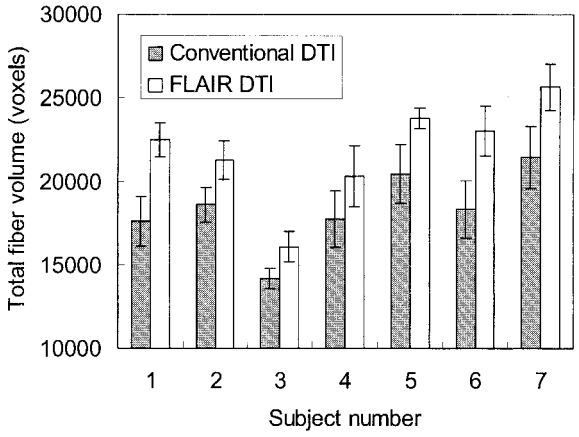

FIG 5. Comparison of total volumes of fibers tracked on conventional DTI versus FLAIR DTI. For all subjects, FLAIR DTI depicted significantly more tracts than conventional DTI, with individual P values of .001–.02 (Student t test; $n = 5$ for each individual). On average, about 17% additional fiber tracts were detected on FLAIR DTI. The group difference was also significant ($P < .0005$, paired Student t test; $n = 7$).

which consistently showed higher FA with FLAIR DTI (4–6).

The existence of pulsatile CSF flow may lead to incomplete CSF suppression in FLAIR, especially in regions showing rapid CSF flow, such as the posterior fossa and the basal cisterns (12, 22). Under such circumstances, the efficacy of FLAIR DTI to eliminate CSF partial volume effects is reduced. Nevertheless, even with incomplete CSF suppression, the CSF signal intensity on FLAIR images is substantially lower than that on conventional DTI (12, 22). Therefore, the decrease in the contributions of CSF to anisotropy measurements on FLAIR DTI should still be helpful. Alternative FLAIR imaging schemes (23–25) are immune to pulsatile CSF flow; these schemes could potentially be incorporated into FLAIR DTI to further suppress CSF signals.

On the contrary, in regions relatively free of CSF contamination, conventional DTI is advantageous in providing source images with an SNR higher than that of FLAIR images. Previous reports have documented the efficacy of FLAIR in ADC or FA measurements in healthy and diseased brain (3–6). However, they did not address issues related to white matter tractography, which could possibly be affected with reduced SNR. Although SNR may not be critical in terms of ADC calculation, a low SNR is known to increase the uncertainty in the direction determination of the major eigenvector of the diffusion tensor (26, 27). The consequent errors that could hamper successful fiber tracking (9) and must therefore be investigated. Minor false tracts were occasionally found on FLAIR tractograms, possibly the result of inferior SNR that led to uncertainty in the derivation of the direction of major eigenvectors. That is to say, tractography with FLAIR DTI tends to be more sensitive in detecting fibers near the CSF spaces, whereas tractography with conventional DTI seems to give higher specificity due to better SNR. Fortunately, the influence from noise is random by nature. In regions of adjacent voxels showing highly consistent fiber orientations (i.e., where the major neural fiber pathways are), the presence of noise would result in only increased directional deviations, causing fewer tracts to be found (26, 27). On the other hand, in regions of adjacent voxels showing inconsistent fiber orientations, the occurrence of false tracts on FLAIR DTI entails an incidental directional consistency due to random noise. In other words, false tracts due to noise could occur only with a low probability, as seen in our study in which the minor false tracts appeared to be irrelevantly regional, with no connections found with other major fiber bundles. As a result, tracking of major white matter tracts when seed points had been specifically located did not seem to be affected in a noticeable manner, making false fiber tracts in FLAIR DTI less of a concern. By the same rule, it is reasonable to believe that the increased volume of fibers tracts found on FLAIR DTI was due to elimination of CSF partial volume effects but not because of the increased noise.

Our results show that the FLAIR method is superior to conventional DTI in white matter tractography, especially in terms of eliminating CSF partial volume effects. The drawback is reduced SNR with FLAIR DTI in regions relatively free of CSF contamination, although it admittedly results in the estimation uncertainty for the FA or the direction of the major eigenvector of the diffusion tensor, does not seem to be a major obstacle for successful fiber trac-

tography. The FLAIR technique, however, has an imaging time intrinsically longer than that of conventional DTI due to long TR (several T1s) needed for complete recovery of the longitudinal magnetization plus a long TI (about 2 seconds) for effective CSF suppression. The longer time for FLAIR DTI did not cause observable disadvantages in our study because we recruited healthy subjects who were highly cooperative during image acquisition; therefore, subject motion was not an important concern. In reality, however, involuntary motion, such as respiration or brain motion (28) of uncooperative patients, may lead to image blurring particularly at the boundaries of the brain. Although we did not investigate the effect of motion, it should be taken into consideration when the DTI protocol is set up in routine clinical practice. In our implementation, the two-step image acquisition for odd- and even-numbered sections further lengthens the total imaging time for FLAIR DTI by a factor of 2. We are currently implementing an alternative version of FLAIR that incorporates an interleaving scheme for the odd- and even-numbered sections within one TR to partially resolve the concern about imaging time.

Conclusion

FLAIR DTI helps to improve white matter tractography by eliminating CSF partial volume effects. Despite its reduced SNR and longer imaging time, FLAIR DTI should be used for white matter tractography when brain regions prone to CSF contamination are of clinical interest.

References

1. Le Bihan D, Mangin JF, Poupon C, et al. **Diffusion tensor imaging: concepts and applications.** *J Magn Reson Imaging* 2001;13:534–546
2. Mori S, Crain BJ, Chacko VP, van Zijl PC. **Three-dimensional tracking of axonal projections in the brain by magnetic resonance imaging.** *Ann Neurol* 1999;45:265–269
3. Latour LL, Warach S. **Cerebral spinal fluid contamination of the measurement of the apparent diffusion coefficient of water in acute stroke.** *Magn Reson Med* 2002;48:478–486
4. Hirsch JG, Bock M, Essig M, Schad LR. **Comparison of diffusion anisotropy measurements in combination with the flair-technique.** *Magn Reson Imaging* 1999;17:705–716
5. Papadakis NG, Martin KM, Mustafa MH, et al. **Study of the effect of CSF suppression on white matter diffusion anisotropy mapping of healthy human brain.** *Magn Reson Med* 2002;48:394–398
6. Ma X, Kadah YM, LaConte SM, Hu X. **Enhancing measured diffusion anisotropy in gray matter by eliminating CSF contamination with FLAIR.** *Magn Reson Med* 2004;51:423–427
7. Kwong KK, McKinstry RC, Chien D, Crawley AP, Pearlman JD, Rosen BR. **CSF-suppressed quantitative single-shot diffusion imaging.** *Magn Reson Med* 1991;21:157–163
8. Falconer JC, Narayana PA. **Cerebrospinal fluid-suppressed high-resolution diffusion imaging of human brain.** *Magn Reson Med* 1997;37:119–123
9. Basser PJ, Pajevic S, Pierpaoli C, Duda J, Aldroubi A. **In vivo fiber tractography using DT-MRI data.** *Magn Reson Med* 2000;44:625–632
10. Reese TG, Heid O, Weisskoff RM, Wedeen VJ. **Reduction of eddy-current-induced distortion in diffusion MRI using a twice-refocused spin echo.** *Magn Reson Med* 2003;49:177–182
11. Alexander AL, Tsuruda JS, Parker DL. **Elimination of eddy current artifacts in diffusion-weighted echo-planar images: the use of bipolar gradients.** *Magn Reson Med* 1997;38:1016–1021
12. Wu HM, Yousem DM, Chung HW, Guo WY, Chang CY, Chen CY. **Influence of scanning parameters on high-intensity CSF artifacts in fast-FLAIR imaging.** *AJNR Am J Neuroradiol* 2002;23:393–399
13. Henkelman RM. **Measurement of signal intensities in the presence of noise in MR images.** *Med Phys* 1985;12:232–233
14. Basser PJ, Pierpaoli C. **A simplified method to measure the diffusion tensor from seven MR images.** *Magn Reson Med* 1998;39:928–934
15. Papadakis NG, Xing D, Houston GC, et al. **A study of rotationally invariant and symmetric indices of diffusion anisotropy.** *Magn Reson Imaging* 1999;17:881–892
16. Terajima K, Nakada T. **EZ-tracing: a new ready-to-use algorithm for magnetic resonance tractography.** *J Neurosci Methods* 2002;116:147–155
17. Lazar M, Weinstein DM, Tsuruda JS, et al. **White matter tractography using diffusion tensor deflection.** *Hum Brain Mapp* 2003;18:306–321
18. Kier EL, Staib LH, Davis LM, Bronen RA. **Anatomic dissection tractography: a new method for precise MR localization of white matter tracts.** *AJNR Am J Neuroradiol* 2004;25:670–676
19. Arfanakis K, Haughton VM, Carew JD, Rogers BP, Dempsey RJ, Meyerand ME. **Diffusion tensor MR imaging in diffuse axonal injury.** *AJNR Am J Neuroradiol* 2002;23:794–802
20. Watts R, Liston C, Niogi S, Ulug AM. **Fiber tracking using magnetic resonance diffusion tensor imaging and its applications to human brain development.** *Ment Retard Dev Disabil Res Rev* 2003;9:168–177
21. Pierpaoli C, Barnett A, Pajevic S, et al. **Water diffusion changes in Wallerian degeneration and their dependence on white matter architecture.** *Neuroimage* 2001;13:1174–1185
22. Bakshi R, Caruthers SD, Janardhan V, Wasay M. **Intraventricular CSF pulsation artifact on fast fluid-attenuated inversion-recovery MR images: analysis of 100 consecutive normal studies.** *AJNR Am J Neuroradiol* 2000;21:503–508
23. Herlihy AH, Hajnal JV, Curati WL, et al. **Reduction of CSF and blood flow artifacts on FLAIR images of the brain with k-space reordered by inversion time at each slice position (KRISP).** *AJNR Am J Neuroradiol* 2001;22:896–904
24. Herlihy AH, Oatridge A, Curati WL, Puri BK, Bydder GM, Hajnal JV. **FLAIR imaging using nonselective inversion pulses combined with slice excitation order cycling and k-space reordering to reduce flow artifacts.** *Magn Reson Med* 2001;46:354–364
25. Tanaka N, Abe T, Kojima K, Nishimura H, Hayabuchi N. **Applicability and advantages of flow artifact-insensitive fluid-attenuated inversion-recovery MR sequences for imaging the posterior fossa.** *AJNR Am J Neuroradiol* 2000;21:1095–1098
26. Jones DK. **Determining and visualizing uncertainty in estimates of fiber orientation from diffusion tensor MRI.** *Magn Reson Med* 2003;49:7–12
27. Basser PJ, Pajevic S. **Statistical artifacts in diffusion tensor MRI (DT-MRI) caused by background noise.** *Magn Reson Med* 2000;44:41–50
28. Enzmann DR, Pelc NJ. **Brain motion: measurement with phase-contrast MR imaging.** *Radiology* 1992;185:653–660